Bremsstrahlung In High Density Mediums

Mert Yücemöz[1]

[1]University of Bath

Key Points:

- Different mediums create another new asymmetry and cause new asymmetric bremsstrahlung asymmetry, R about the line perpendicular to the direction of motion.
- Higher the density of the medium, slower the EM wave speed, higher radiation bend and higher the bremsstrahlung asymmetry in the forward peaking compared to backward peaking.
- Higher density medium causes backward peaking radiation length to decrease.

Corresponding author: Mert Yucemoz, m.yucemoz@bath.ac.uk

Abstract

Previously the radiation patterns of combined parallel and perpendicular motions from the accelerated relativistic particle at low and high frequencies of the bremsstrahlung process with an external lightning electric field were explained. The primary outcome was that radiation patterns have four relative maxima with two forward peaking and two backward peaking lobes. The asymmetry of the radiation pattern, i.e., the different intensities of forwarding and backward peaking lobes, is caused by the Doppler effect. A novel outcome is that bremsstrahlung has an asymmetry of the four maxima around the velocity vector caused by the curvature of the particle's trajectory as it emits radiation. This extended work reports another novel asymmetry in the overall radiation pattern. Previously stated bremsstrahlung asymmetry, R was an asymmetry in the radiation lobe pairs about particles velocity vector. Bremsstrahlung asymmetry used to occur at the same level in both forward radiation lobe pairs and backward radiation lobe pairs. However, in high-density mediums where the emitted wave can lag behind the speed of the particle, symmetry of the magnitude of bremsstrahlung asymmetry, R differs between forward peaking radiation lobe pairs relative to backward peaking radiation lobe pairs. This is another novel asymmetry and it causes bremsstrahlung asymmetry, R to be larger in the forward peaking compared to backward peaking radiation. The outcome is the shrink in radiation length that occurs in the backward peaking lobes. This extended mathematical modeling of the bremsstrahlung process into different high-density mediums helps to better understand the physical processes of a single particle's radiation pattern, which might assist the interpretation of observations with networks of radio receivers and arrays of γ-ray detectors.

1 Introduction

Bremsstrahlung radiation patterns were predicted to be forward and backward peaking with associated novel bremsstrahlung asymmetry, R (Yücemöz & Füllekrug, 2021). In addition, the time evolution of dipole radiation pattern into forward-backward peaking was demonstrated. The reasoning for the existence of forward-backward peaking due to the collapse and separation of the lobes of the dipole radiation pattern was associated with the conservation of symmetry axes (Yücemöz & Füllekrug, 2021). Furthermore, this extended modelling of the bremsstrahlung process into high-density mediums, reveals a new outcome that symmetry of the bremsstrahlung asymmetry, R about the axis perpendicular to the direction of particle's motion, between forward and backward peaking side is broken. Increasing refractive index causes bremsstrahlung asymmetry, R to exist at different ratios between forward and backward peaking radiation lobe pairs. Increasing refractive index increases the bremsstrahlung asymmetry between the front radiation lobe pairs compared to backward radiation lobe pairs. Furthermore, increasing the refractive index shortens the radiation length in the backward peaking radiation side.

1.1 Aims & Objectives

This theoretical approach aims to extend the previous bremsstrahlung model to different high-density mediums where particle speed can exceed the speed of an emitted electromagnetic wave. In addition, to predict and understand how radiation patterns and previously introduced bremsstrahlung asymmetry parameter R changes within these high refractive index mediums. To achieve the stated aim, particle emitted frequency-dependent refractive index, $n(\omega)$ is identified, expressed in terms of Solid angle, $\Omega_{n,\beta}$, (Eq. 12) and substituted into the main radiation pattern equation (Eq. 13).

2 Equation Relating Top and Bottom Radiation lobes Together Using Bremsstrahlung Asymmetry, R

Considering forward peaking part of the overall radiation pattern. Radiation intensity, I of top lobe (I_T) can be related to the bottom lobe (I_B) with bremsstrahlung asymmetry,R mathematically by

$$I_T = \frac{I_B}{(1-R)} \tag{1}$$

This information can be used to find the bremsstrahlung angle, θ_{Brem} between the two forward peaking radiation lobes that are bremsstrahlung asymmetric, with asymmetry value R.

By knowing the distance, Ξ(m) between the maximum points of two radiation intensities, I in the forward peaking lobes, bremsstrahlung angle between the two forward peaking lobes can be written as,

$$cos(\theta_{Brem}) = \frac{I_T^2 + I_B^2 - \Xi^2}{2 I_T I_B} \tag{2}$$

The equation 1 and 2 can also be used for backward peaking radiation lobes.

3 Extending Bremsstrahlung modelling to High Density Mediums

The equation for translating the angular frequency of the emitted wave into the laboratory frame for the Doppler shift is given by (Jackson, 1999, p. 720, eq. 15.40).

$$\omega^{'} = \gamma\omega(S_{SpecialR} - \beta S_{SpecialR} cos(\theta_{n,\beta})). \tag{3}$$

$\theta_{n,\beta}$ is the angle between the emitted radiation unit vector and the particle velocity vector.

Previously, bremsstrahlung radiation pattern with bremsstrahlung asymmetry, R is given by (Yücemöz & Füllekrug, 2021)

$$\frac{d^2I}{d\omega\Omega_{rad}} = \frac{z^2e^2(\gamma\omega(S_{SpecialR} - \beta S_{SpecialR} cos(\theta_{n,\beta}))^2}{4\pi^2 c\epsilon_0}\left| sin(\theta_{n,\beta})\left[- \frac{s_{fv} s_f z (s_{ft})^{1.461} 4.365 \times 10^{26}}{c} \left[\pi^{1/2} 2^{-(1/2)\nu_1} \alpha^{-\nu_1 - 1} e^{-\frac{y^2\alpha^{-2}}{8}} \times D_{\nu_1}(2^{-1/2}\alpha^{-1}y)\right] + \frac{s_{fv} z s_f (s_{ft})^{1.5} 1.565 \times 10^{27}}{c}\left[\pi^{1/2} 2^{-(1/2)\nu_2} \alpha^{-\nu_2 - 1} e^{-\frac{y^2\alpha^{-2}}{8}} \times D_{\nu_2}(2^{-1/2}\alpha^{-1}y)\right]\right]\right|^2, \tag{4}$$

where R is the bremsstrahlung asymmetry control parameter, which plays a crucial role in distinguishing the parameter y from α. $D_v(z)$ is the parabolic cylinder function.

The parabolic cylinder function is given by (Whittaker & Watson, 1927, p. 347)

$$D_v(z) = 2^{v/2+1/4} z^{-1/2} W_{v/2+1/4,1/4}(1/2z^2), \tag{5}$$

where, $W_{v/2+1/4,1/4}(1/2z^2)$ is a Whittaker function (Whittaker & Watson, 1927, p. 346) and

$$W_{\kappa,\mu}(1/2z^2) = \frac{\Gamma(-2\mu)M_{\kappa,\mu}(1/2z^2)}{\Gamma(1/2-\mu-\kappa)} + \frac{\Gamma(2\mu)M_{\kappa,-\mu}(1/2z^2)}{\Gamma(1/2+\mu-\kappa)}, \tag{6}$$

where, $M_{\kappa,\mu}(1/2z^2)$ is another Whittaker function (Kiyosi Ito and The Mathematical Society of Japan, 1993) & (Whittaker & Watson, 1927, p. 347) and

$$M_{\kappa,\mu}(1/2z^2) = {}_1F_1(1/2+\mu-\kappa; 2\mu+1; 1/2z^2)(1/2z^2)^{1/2+\mu}e^{-1/21/2z^2}. \tag{7}$$

For the second term of equation (27) with Whittaker M function of negative μ

$$M_{\kappa,-\mu}(1/2z^2) = {}_1F_1(\mu-\kappa; 2\mu; 1/2z^2)(1/2z^2)^{1/2+\mu}e^{-1/21/2z^2}, \tag{8}$$

where ${}_1F_1(1/2+\mu-\kappa; 2\mu+1; z)$ is a confluent hypergeometric function of the first kind (Abramowitz & Stegun, 1972) and

$${}_1F_1(1/2+\mu-\kappa; 2\mu+1; 1/2z^2) = \frac{U_{\kappa,\mu}(1/2z^2)}{e^{-1/2z^2/2}(1/2z^2)^{\mu+1/2}}, \tag{9}$$

where, $U_{\kappa,\mu}(\frac{z^2}{2})$ is the confluent hypergeometric function of the second kind, named Kummer's U function such that

$$U_{\kappa,\mu}(\frac{z^2}{2}) = (\frac{z^2}{2})^{\mu+1/2}e^{-\frac{z^2}{4}}\sum_{n=0}^{\infty}\frac{(m-k+1/2)_n}{n!(2\mu+1)_n}\left(\frac{z^2}{2}\right)^n. \tag{10}$$

Where the constant quantities z, κ and μ are defined as $z = 2^{-1/2}\alpha^{-1}y$, $\kappa = v/2+1/4$, $\mu = 1/4$.

Transforming equation 4 into a form that allows to predict how radiation pattern would be affected in a denser medium where electromagnetic wave speed can slow down below particle speed. This can be done by dividing speed of light in vacuum by frequency dependent refractive index n(ω).

Every speed of light in vacuum "c" parameter can be replaced with "$\frac{c}{n(\omega)}$".

Therefore,

$$\frac{c}{n(\omega)} = \frac{c}{\sqrt{\epsilon_r\mu_r}} = \frac{c}{\sqrt{\left(1-\frac{i\sigma}{\epsilon_0\omega'}\right)\mu_r}} \tag{11}$$

From equation 3, we can transform angular wave frequency from moving frame of reference, $\omega^{'}$ to laboratory frame of reference, ω in equation 13.

$$\frac{c}{\sqrt{\left(1-\frac{i\sigma}{\epsilon_0\omega'}\right)\mu_r}} = \frac{c}{\sqrt{\left(1-\frac{i\sigma}{\epsilon_0\left[\gamma\omega(S_{SpecialR}-\beta S_{SpecialR}cos(\theta_{n,\beta}))\right]}\right)\mu_r}} \tag{12}$$

Where σ is the electrical conductivity of the medium. Hence,

$$\frac{d^2I}{d\omega\Omega_{rad}} = \frac{z^2e^2(\gamma\omega(S_{SpecialR} - \beta S_{SpecialR}cos(\theta_{n,\beta}))^2}{4\pi^2c\epsilon_0}\Bigg|sin(\theta_{n,\beta})$$
$$\Bigg[-\frac{s_{fv}s_fz(s_{ft})^{1.461}4.365\times10^{26}}{\frac{c}{\sqrt{\left(1-\frac{i\sigma}{\epsilon_0\left[\gamma\omega(S_{SpecialR}-\beta S_{SpecialR}cos(\theta_{n,\beta}))\right]}\right)\mu_r}}}$$
$$\left[\pi^{1/2}2^{-(1/2)\nu_1}\alpha^{-\nu_1-1}e^{-\frac{y^2\alpha^{-2}}{8}}\times D_{\nu_1}(2^{-1/2}\alpha^{-1}y)\right]+$$
$$\frac{s_{fv}zs_f(s_{ft})^{1.5}1.565\times10^{27}}{\frac{c}{\sqrt{\left(1-\frac{i\sigma}{\epsilon_0\left[\gamma\omega(S_{SpecialR}-\beta S_{SpecialR}cos(\theta_{n,\beta}))\right]}\right)\mu_r}}}\left[\pi^{1/2}2^{-(1/2)\nu_2}\alpha^{-\nu_2-1}e^{-\frac{y^2\alpha^{-2}}{8}}\times D_{\nu_2}(2^{-1/2}\alpha^{-1}y)\right]\Bigg]\Bigg|^2, \tag{13}$$

where the Lorentz factor γ is $\gamma = \frac{1}{\sqrt{1-\beta^2}}$ (dimensionless), and ω is the received angular frequency in the laboratory (stationary) frame of reference in rad/s. In addition, the new definition of α is $\alpha^2 = \frac{b^R(\gamma\omega(S_{SpecialR}-\beta S_{SpecialR}cos(\theta_{n,\beta})))^R(sin(\theta_{n,\beta}))^R}{(\tau^R)^2\left[\frac{c}{\sqrt{\left(1-\frac{i\sigma}{\epsilon_0\left[\gamma\omega(S_{SpecialR}-\beta S_{SpecialR}cos(\theta_{n,\beta}))\right]}\right)\mu_r}}\right]^R}$ $[s^{-2}]$, and the new definition of y is $y = \frac{\gamma\omega(S_{SpecialR}-\beta S_{SpecialR}cos(\theta_{n,\beta}))sin(\theta_{n,\beta})a}{\left[\frac{c}{\sqrt{\left(1-\frac{i\sigma}{\epsilon_0\left[\gamma\omega(S_{SpecialR}-\beta S_{SpecialR}cos(\theta_{n,\beta}))\right]}\right)\mu_r}}\right]\tau}$ $[\mathrm{s}^{-1}]$.

4 Results

This section presents previous prediction of high frequency radiation pattern of a single electron with bremsstrahlung, R and doppler frequency asymmetry accelerated under an external lightning leader tip electric field using the derived equation 4. In addition, results extend (Eq. 13) to demonstrate what would happen to radiation length and novel bremsstrahlung asymmetry, R if bremsstrahlung process takes place inside a high density medium.

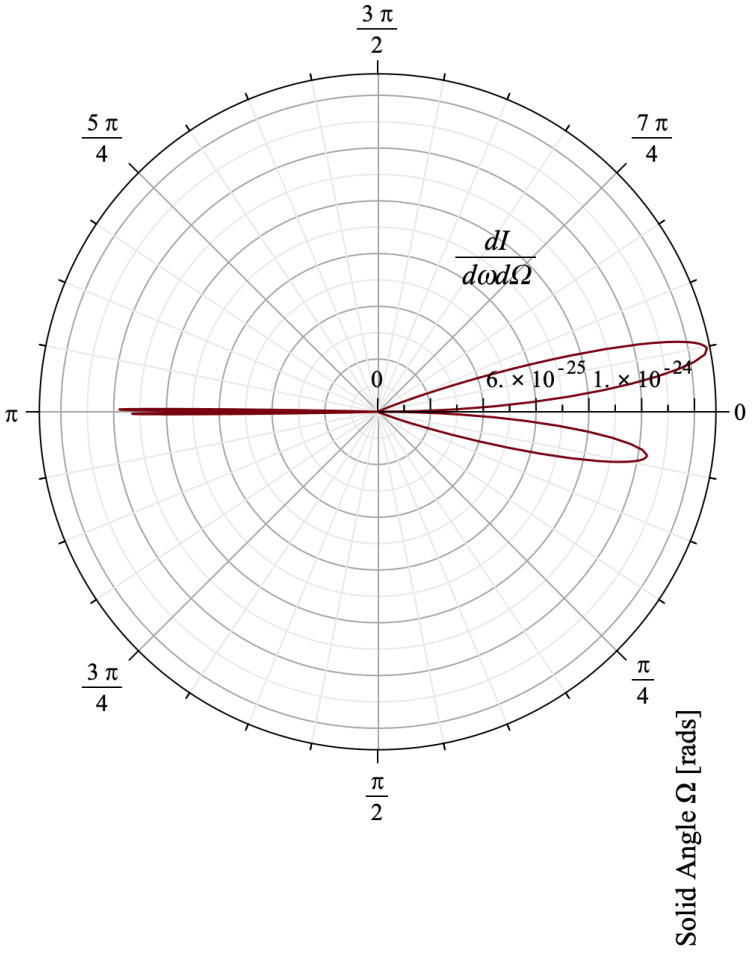

Figure 1. The Radiation patterns are emitted by the anti-clockwise rotating charged particle - bremsstrahlung process. High density (particle travelling inside the water) medium causes a novel asymmetry about a line perpendicular to the direction of motion of a particle. This novel asymmetry causes bremsstrahlung asymmetry, R to occur at different proportions in forward and backward peaking lobe pairs. Therefore, bremsstrahlung asymmetry, R is higher in forward peaking radiation and lower in backward peaking radiation. Moreover, a high-density medium also causes radiation length to shorten in backward peaking radiation. Plot is in Polar co-ordinates. Horizontal axis gives the radiation intensity per Solid angle, Ω, per emitted angular radiation frequency, ω. In addition, angle of the Polar plot is the Solid angle, Ω. The values used for plotting are: mean free time τ= 30 μs, number of charges z= 1, a=100 μm, b= 1 nm (a and b are related to mean free path), s_{ft}= 1, s_f= 1, $S_{SpecialR}$ = 1, velocity-time scaling factor s_{ftv}= 1×10^9 and velocity scaling factor s_{fv}= 8.19 ×10^{-11}. Finally, the bremsstrahlung asymmetry is R= 1/8. In addition, $\frac{1}{9} \leq R \leq \frac{1}{3}$., medium conductivity, σ = 0.005, relative permeability, μ_r = 0.99

A high-density medium for a single electron is chosen to be water. As can be seen in figure 1, as the bremsstrahlung electron travels inside water following a curved trajectory, a high-density medium causes larger bremsstrahlung asymmetry in the forward peaking radiation. This difference in the magnitude of bremsstrahlung asymmetry, R in forward and backward peaking radiation is a novel asymmetry in the radiation pattern. High-density medium also causes backward peaking radiation length to decrease.

5 Summary

In summary, the bremsstrahlung process occurring in a high-density medium causes bremsstrahlung asymmetry, R to be a different magnitude in forward and backward peaking radiation direction. This difference in bremsstrahlung asymmetry, R is a novel asymmetry in radiation pattern. Bremsstrahlung asymmetry was found to occur at a larger magnitude in a forward direction with a larger bremsstrahlung asymmetry, R number. Finally, radiation length in a high-density medium of the bremsstrahlung process was found to be shorter in the backward peaking radiation. Top and bottom radiation intensities are related to each other by the bremsstrahlung asymmetry parameter R given in the equation 1.

Acknowledgments

EPSRC and MetOffice sponsor my PhD project under contract numbers EG-EE1239 and EG-EE1077. I would like to thank a lot to my family for their support and good wishes. The Maple worksheets used to simulate the particle trajectory, external lightning leader tip electric field, particle velocity, and the radiation patterns are openly available from the University of Bath Research Data Archive.

References

Abramowitz, M., & Stegun, I. A. (1972). Handbook of Mathematical Functions: with Formulas, Graphs, and Mathematical Tables. In (10th ed., Vol. National Bureau of Standards Applied mathematics series 55, p. 1046). Washington, D.C. , USA: U.S. Dept. of Commerce : U.S. G.P.O. (ISBN: 9781591242178)

Jackson, J. D. (1999). Classical Electrodynamics. In (3rd ed., p. 661-732). New York, United States: John Wiley & Sons, Inc. (ISBN:9780471309321) doi: 10.1002/3527600434.eap109

Kiyosi Ito and The Mathematical Society of Japan. (1993). Encyclopedic Dictionary of Mathematics. In (2nd ed., Vol. 1, p. 2168). London, England: The MIT Press. (ISBN: 0262590204)

Whittaker, E. T., & Watson, G. N. (1927). A course in modern analysis : an introduction to the general theory of infinite processes and of analytical functions, with an account of the principal transcendental functions. In (4th ed., p. 616). The Pitt Building, Trumpington Street, Cambridge, CB2 1RP: Cambridge University Press. (ISBN: 0521091896)

Yücemöz, M., & Füllekrug, M. (2021). Asymmetric backward peaking radiation pattern from a relativistic particle accelerated by lightning leader tip electric field. *Journal of Geophysical Research: Atmospheres*, *126*(13), e2020JD033204. Retrieved from `https://agupubs.onlinelibrary.wiley.com/doi/abs/10.1029/2020JD033204` (e2020JD033204 2020JD033204) doi: https://doi.org/10.1029/2020JD033204